Biological Conservation 313 (2026) 111574

Contents lists available at ScienceDirect

Biological Conservation

journal homepage: www.elsevier.com/locate/biocon

Mesoscale ocean dynamics structure fisheries interaction risk for an endangered seabird

Ho Fung Wong [a,*], David Schoeman [a,h], Peter I. Miller [b], Lily Bentley [c], Luke Halpin [d,e], Johannes H. Fischer [f], Igor Debski [f], Samhita Bose [f], Graeme Elliott [f,g], Kath Walker [f,g], Kylie L. Scales [a]

[a] Ocean Futures Research Cluster, School of Science, Technology & Engineering, University of the Sunshine Coast, 90 Sippy Downs Dr, Sippy Downs, QLD 4556, Queensland, Australia
[b] Remote Sensing Group, Plymouth Marine Laboratory, Prospect Pl, Plymouth, PL1 3DH, United Kingdom
[c] Centre for Biodiversity and Conservation Science, University of Queensland, Goddard Building, University Drive, St Lucia, QLD 4072, Queensland, Australia
[d] Gulbali Research Institute, Charles Sturt University, Albury, NSW, 2640, Australia
[e] Halpin Wildlife Research, Vancouver, British Columbia, Canada
[f] Biodiversity systems and Aquatic Unit, Department of Conservation, Aotearoa, New Zealand
[g] Terrestrial Biodiversity Unit, Department of Conservation, Aotearoa, New Zealand
[h] Centre for African Conservation Ecology, Nelson Mandela University, Gqeberha, South Africa

ARTICLE INFO

Keywords:
Fisheries bycatch
Marine megafauna
Oceanography
Spatial modelling
Dynamic ocean management
Antipodean albatross
Endangered seabirds

ABSTRACT

Fisheries bycatch poses a major threat to marine predators and remains a global challenge to sustainable fisheries. Conservation and management strategies can be informed by identifying zones of overlap between fishing effort and threatened, endangered or protected species, or existing bycatch hotspots. However, few studies have incorporated ocean data and the age and sex classes of seabirds into these assessments. Here, we examined the environmental conditions that drive fisheries interaction risk for the endangered Antipodean albatross (*Diomedea antipodensis antipodensis*). Specifically, we assessed interaction risk by combining satellite-tracking data from 192 individuals across age and sex classes of all life stages with data from the Automatic Identification System (AIS) vessel-tracking program. The integration of satellite-tracking and oceanographic data facilitated assessment of how physical ocean features — such as recurring thermal fronts, turbulent ocean mixing, and swirling eddies — shaped high-risk interaction zones. Hotspots of interaction risk spanned from 25°S to 40°S and varied seasonally. Overall, interaction risk was significantly higher during May–August and among juveniles. Over broad climatological scales, the interaction risk was greatest where thermal fronts occur frequently. At finer scales, interaction risk was intensified in association with aggregative Lagrangian Coherent Structures. These findings suggest that Regional Fisheries Management Organisations could take immediate action, such as extending current bycatch mitigation measures to include fishing grounds between 25 and 30°S, to cover the hotspots for juvenile and female seasonally. Incorporating measures of mesoscale ocean dynamics in delineating zones of interaction risk for species of conservation concern provides a potential step forward for dynamic threat management.

1. Introduction

Globally, commercial fisheries exert a range of pressures on marine ecosystems (Pauly et al., 2005). One of the suchpressures often arise when there is interaction between fisheries and non-target marine wildlife (Liu et al., 2019; Jog et al., 2022). In some systems, marine predators such as seabirds can benefit from these interactions by accessing supplementary food sources through depredation of baited fishing lines or consumption of catch or discards (Votier et al., 2004; Granadeiro et al., 2014; Corbeau et al., 2021). However, interactions

* Corresponding author at: 90 Sippy Downs Dr, Sippy Downs, QLD 4556, Queensland, Australia.
E-mail addresses: Hofung.wong@research.usc.edu.au (H.F. Wong), dschoema@usc.edu.au (D. Schoeman), PIM@pml.ac.uk (P.I. Miller), l.bentley@uq.edu.au (L. Bentley), jfischer@doc.govt.nz (J.H. Fischer), idebski@doc.govt.nz (I. Debski), samhita.bose@wcc.govt.nz (S. Bose), gelliott@doc.govt.nz (G. Elliott), kwalker@doc.govt.nz (K. Walker), kscales@usc.edu.au (K.L. Scales).

https://doi.org/10.1016/j.biocon.2025.111574
Received 2 June 2025; Received in revised form 13 October 2025; Accepted 19 October 2025
Available online 27 October 2025

also result in the risk of fisheries bycatch (i.e., the capture of non-target species) and competition for food (Read et al., 2006; Bugoni et al., 2010; Cury et al., 2011; Grémillet et al., 2008; Corbeau et al., 2021).

Fisheries bycatch is a major threat to many populations of marine predators of conservation concern (Avila et al., 2018; Jog et al., 2022), contributing to population declines in sea turtles (Lewison et al., 2014), marine mammals (Güçlüsoy, 2008; Slooten and Dawson, 2010; Marsh and O'Shea, 2011; Lewison et al., 2014; Brough et al., 2019) and seabirds (Anderson et al., 2011; Croxall et al., 2013), particularly albatrosses, petrels and shearwaters (Anderson et al., 2011; Phillips et al., 2016). An estimated 50,000 to 75,000 seabirds are known to be killed by pelagic longline fisheries each year, with an estimated 170 million individuals exposed to fisheries bycatch (Anderson et al., 2011; Dias et al., 2019). In particular, 40,000 individuals from 26 species of albatross and petrel are estimated to be caught annually in the Southern Hemisphere (Abraham et al., 2019). Up to 90 % of albatross species are threatened by fisheries bycatch (Dias et al., 2019), including wandering albatross (*Diomedea exulans*), black-browed albatross (*Thalassarche melanophrys*), black-footed albatross (*Phoebastria nigripes*), Amsterdam albatross (*D. amsterdamensis*), and Tristan albatross (*D. dabbenena*) (Arnold et al., 2006; Véran et al., 2007; Wanless et al., 2009; Rivalan et al., 2010; Anderson et al., 2011; Croxall et al., 2013).

Studies of seabird–fisheries interactions that focus on spatial overlap between fishing effort and seabird distribution can provide insights useful for managing bycatch risk (Clay et al., 2019; Carneiro et al., 2020). Recently, the expanded use of both animal- and vessel-tracking technologies has yielded new insight into seabird–fisheries interactions by providing new and more detailed information on seabird movement and distribution. For example, hotspots of seabird–fisheries overlap have been identified by examining the respective distributions of seabird-tracking locations and fishing efforts from logbooks (Clay et al., 2019; Carneiro et al., 2020). Such seabird–fisheries overlap studies have been further facilitated by the availability of more precise fishing locations derived from vessel-based Automatic Identification Systems (AIS) (Corbeau et al., 2021; Cruz et al., 2022) and birds equipped with radar-detecting tags that can directly sense vessels in the vicinity (Weimerskirch et al., 2018; Navarro-Herrero et al., 2024).

From this foundation of mapping and quantifying interaction risk based on location data only (Copello et al., 2014; Clay et al., 2019; Carneiro et al., 2020), the incorporation of biophysical ocean data would benefit risk assessments by improving our understanding of the spatial drivers of risk hotspots and potentially enable dynamic threat management for species (Hazen et al., 2018). Due to the dynamic nature of the ocean, management is complicated (Lewison et al., 2015). Although the interactions between marine predators and their environment are fluid (Grantham et al., 2011), the use of responsive spatial management strategies could improve the efficiency and efficacy of fisheries management (Maxwell et al., 2012, 2015; Hobday et al., 2011, 2013; Dunn et al., 2016).

The distribution of seabirds varies among sex and age classes, and life history stages (Carneiro et al., 2020), and thus, the impacts of fisheries bycatch vary among these classes. Studies on the bycatch risk of albatrosses and large petrels have focused predominantly on adults (Frankish et al., 2021) and during breeding seasons (Votier et al., 2023). Bycatch risk faced by juveniles and non-breeding adults has been understudied (Gianuca et al., 2017; Carneiro et al., 2020; Frankish et al., 2021; Gimeno et al., 2022; Votier et al., 2023). Among albatrosses, juvenile and immature birds typically comprise more than half of the population (Weimerskirch et al., 1997; Carneiro et al., 2020). The recovery and recruitment of endangered albatrosses could be hindered by high juvenile mortality (Pardo et al., 2017; Carneiro et al., 2020). Therefore, studying the bycatch risk of juveniles has received more attention in recent years, with the intent to inform mitigation measures (Frankish et al., 2021; Votier et al., 2023).

In this study, we examine fisheries-interaction risk for Antipodean albatross arising from pelagic longline fisheries throughout the species' distribution and life cycle. The Antipodean albatross (*Diomedea antipodensis antipodensis)* is a wandering albatross taxon endemic to Aotearoa New Zealand. This species has a highly *K*-selected life strategy (Robertson et al., 2021). Adults of this species breed every second year, as chicks take 12 months to fledge. Fledglings return to the colony after spending six to 11 years at sea, and 50 % start breeding only at the age of 14 (Richard, 2021; Richard et al., 2024). The Antipodean albatross is listed as "Nationally Critical" at a subspecies level by the New Zealand Threat Classification System (Robertson et al., 2021) and "Endangered" by the IUCN Red List of Threatened Species at a species level (which includes the Auckland Island population of Gibson's Albatross *D. a. gibsoni*). The Antipodean albatross has a current population of ~28,000 individuals, which is declining at an estimated 6 % per annum. Bycatch by pelagic longline fisheries in the high seas is considered to be the primary threat to the population (Abraham and Thompson, 2015; Richard and Abraham, 2020; Richard, 2021; Richard et al., 2024).

Here, we aim to identify hotspots and time periods during which fisheries-interaction risk for the Antipodean albatross is highest. In particular, we seek to address important knowledge gaps regarding fisheries interactions for all life-history stages of this endangered population throughout the annual cycle. We explicitly consider the effects of age and sex class or breeding status and use ocean data to model the underlying biophysical drivers of interaction risk, with a particular focus on comparing different mesoscale (i.e., 100 km) physical ocean features (i.e., recurring thermal fronts, turbulent ocean mixing, and swirling eddies). We aim to investigate the influence of bio-physical conditions on the spatial structuring of interaction risk over two distinct spatio-temporal scales: (i) the seasonal variation in the risk of interaction with climatological ocean variables; and (ii) the intensity of interaction risk at monthly timescales with time-matched ocean variables (Fig. 1a).

2. Materials and methods

2.1. Study area

The Antipodean albatross breeds on Moutere Mahue Antipodes Island, Aotearoa New Zealand (49°40′12″S, 178°46′48″E), a Subantarctic island in the South Pacific Ocean (Fig. 1b). The Antipodean albatross has a wide distribution, spanning from western Australia (112°), across the southern Pacific to the Chilean Coast (289°). The study area was set as the full extent of the flight range of our tracked Antipodean albatross population.

2.2. Data collection and processing

2.2.1. Antipodean albatross data

We tracked 192 Antipodean albatrosses across various age and sex classes during 2019–2022 with high-resolution satellite transmitters deployed at their colony. Specifically, we tracked 61 juveniles, 32 female breeders, 26 male breeders, 43 female non-breeders and 30 male non-breeders with satellite transmitters of either ARGOS platform terminal transmitter (PTT) (i.e., Telonics, TAV2630), Global Positioning System (GPS) (i.e., GeoTrak and Icarus) or both (i.e., Wildlife Computers Rainier S20, Lotek Pinpoint, Sextant Technology Sextant, Microwave Telemetry). All individuals were sexed and aged visually at the time of tagging (i.e., between December to March, varied between years) (Elliott & Walker 2019, 2020 and 2022). All tracking devices were attached with waterproof tape onto back feathers (for detailed deployment tagging procedures see Elliott & Walker 2019, 2020 and 2022). The average (± SE) tracking period obtained for these individuals was 191 ± 40.6 days. 44 individuals were tracked across a calendar year, and 24 of them were tracked for >365 days (Table 1). We filtered the collated tracking data by Argos location class quality (0, 1, 2, and 3 (i.e., high quality locations)) to minimise error (Douglas et al., 2012). We also removed successive locations where flight speed exceeded 100 kmph (27.8 ms^{-1}), to eliminate unrealistic locations (Lascelles et al., 2016).

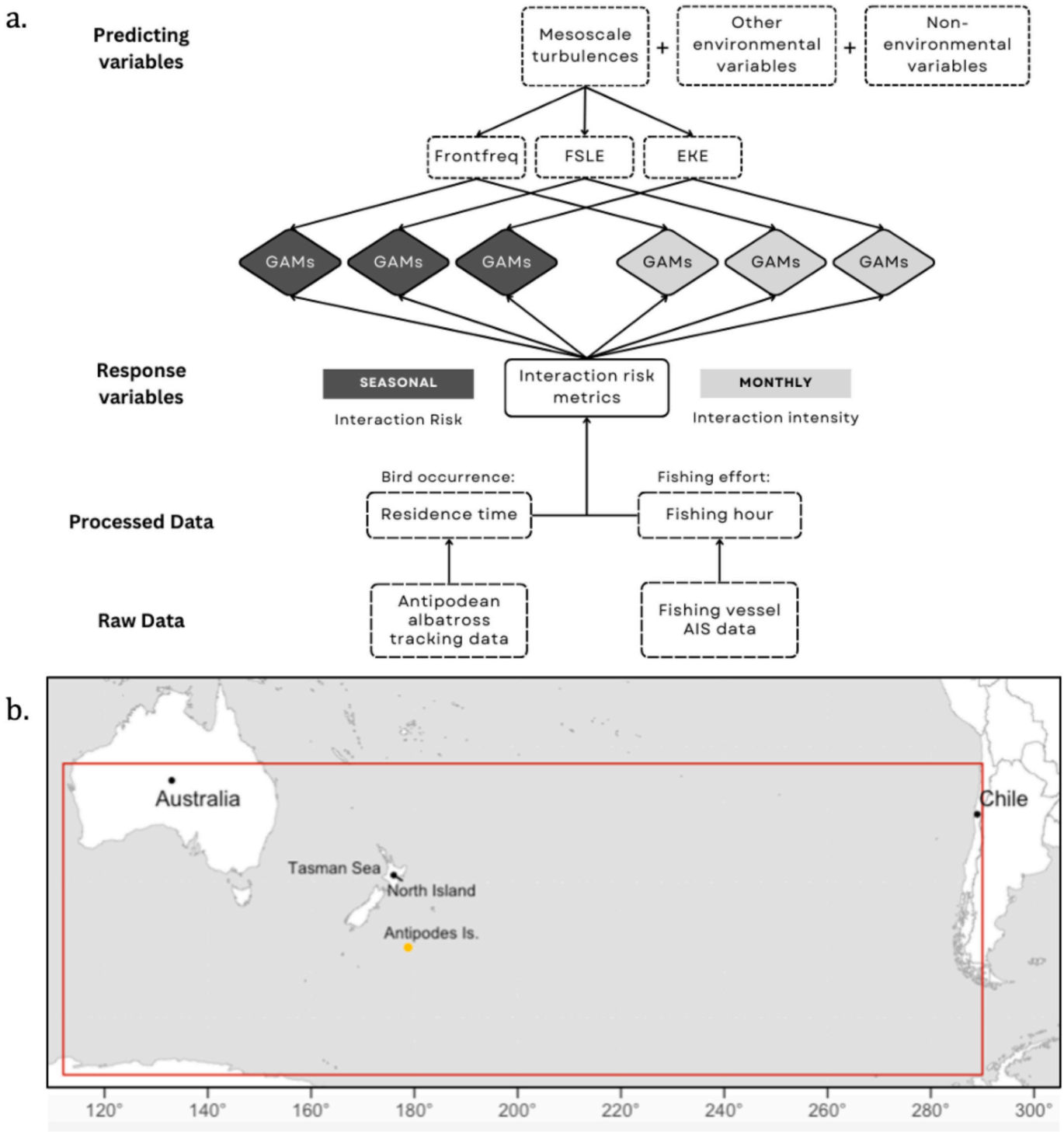

Fig. 1. (a) Schematic flow chart of the study design. A red box indicates the study area. The yellow dot indicates the Antipodean albatross' breeding site — Moutere Mahue Antipodes Island, Aotearoa New Zealand (49°40′12″S, 178°46′48″E). (For interpretation of the references to color in this figure legend, the reader is referred to the web version of this article.)

We then interpolated tracking data linearly at 4-h intervals to obtain a minimum of 6 locations per day using the R package *terra* (Hijmans, 2022).

2.2.2. *Fishing activity data*

For fishing activity, we quantified fishing effort using fishing hours derived from Automatic Identification Systems (AIS) by Global Fishing Watch (GFW; https://globalfishingwatch.org/our-apis/) for the period 2019–2022 (i.e., same period as tracking of Antipodean albatross). GFW detects fishing activity (i.e., fishing hours per grid cell) using a convolutional neural network, which classifies fishing vessels and the period and areas where the vessels are actively fishing (Kroodsma et al., 2018). We selected only pelagic longline fisheries data from the dataset, as these pose the greatest risk to the Antipodean albatross (e.g., Richard et al., 2024). We first calculated the resultant estimate of fishing hours as a metric of fishing effort per 100 km^2 per day using the R package *terra*.

Table 1
Summary of Antipodean albatross tracking data for each year in this study. Twenty-four individuals had tracking days longer than a year. They were counted as a new individual in each year in the summary, with their status remaining unchanged.

Sex	Status	Year	Number of birds	Total number	Mean tracking days (day)	SE (±)
Female	Breeder	2019	4	38	180.6	22.1
		2020	10			
		2021	8			
		2022	16			
	Non-breeder	2019	11	45	156.0	13.8
		2020	19			
		2021	10			
		2022	5			
Male	Breeder	2019	0	28	163.4	16.2
		2020	7			
		2021	11			
		2022	10			
	Non-breeder	2019	8	30	137.3	15.3
		2020	7			
		2021	11			
		2022	4			
Juvenile		2019	20	105	268.6	15.0
		2020	33			
		2021	31			
		2022	21			

We then developed rasters of monthly total fishing hours each year at a 1 × 1° resolution.

2.2.3. Ocean data

We set out this study with a particular focus on comparing different mesoscale (i.e., 100 × 100 km) physical ocean features, such as front frequency, Finite-Size Lyapunov Exponents (FSLE) and eddy kinetic energy (EKE). Front frequency describes how often fronts are detected by estimating the percentage of time a front over a certain threshold (here, 0.1 °C km^{-1}) is observed within each grid cell over a specified period (i.e., weekly, monthly or seasonally) (Miller, 2009). FSLE measures the relative dispersion of particles (i.e., how quickly particles drift apart or toward each other) by tracing them through time-dependent current-velocity fields derived from satellite altimetry (Boffetta et al., 2001; Pardo et al., 2017). It highlights the dynamic transport barriers concentrating particles, nutrients or organisms (i.e., Lagrangian coherent structures (LCS)) that control the horizontal exchange of water into and out of the swirling ocean currents (i.e., eddies) (d'Ovidio et al., 2004). LCS is a useful predictor of fisheries–wildlife interactions in other systems (Cotté et al., 2015; Della Penna et al., 2017; Scales et al., 2018). The EKE is a modelled estimate of eddy intensity, representing the intensification of swirling ocean currents in a given area (Appen et al., 2022).

We derived the monthly and seasonal average of environmental signals of each dynamic variable using four years of data (2019–2022). We first downloaded the raw data (in their native resolution) from online sources (Table 2), including dynamic oceanographic variables such as sea surface temperature (SST; °C), mixed layer depth (MLD; m), salinity (PSU), chlorophyll-*a* concentration (Chl-a; mg/m^3); and mesoscale turbulences such as front frequency (%), FSLE ($days^{-1}$) and EKE (cm^2/s^2) (Table 2.). All environmental variables were re-gridded to the same coordinate system and rasterised to a 1 × 1° resolution using bilinear interpolation using R package *terra* (Hijmans, 2022). We removed salinity because prior inspection revealed a strong positive correlation with SST ($r = 0.757$). Then we calculated the monthly and seasonal median of each environmental variable for each year. Finally, we derived the monthly and seasonal averages of each variable by calculating the median across the four years.

Table 2
Static and dynamic oceanographic variables, resolutions, measurement units and sources.

Variables	Static/dynamic	Class	Units	Native resolution	Sources
Sea surface temperature (SST)	Dynamic	Numeric	°C	0.1°	BRAN2020
Mixed layer depth (MLD)	Dynamic	Numeric	m	0.1°	BRAN2020
Chlorophyll-*a* (Chl-*a*)	Dynamic	Numeric	mg/m^3	4 × 4 km	NASA MODIS
Bathymetry depth (Depth)	Static	Numeric	m	10 arcmin	NOAA
Thermal front frequency (FrontFreq)	Dynamic	Numeric	%	9 × 9 km	Plymouth Marine Laboratory
Finite-Size Lyapunov Exponents (FSLE)	Dynamic	Numeric	$days^{-1}$	0.04°	AVISO+
Eddy kinetic energy (EKE)	Dynamic	Numeric	cm^2/s^2	0.04°	AVISO+
Month/Season	Static	Categorical	/	/	/
Year	Static	Categorical	/	/	/
Sex and age	Static	Categorical	/	/	/
Breeding status	Static	Categorical	/	/	/

2.3. Estimating relative interaction risk and intensity

We estimated interaction risk and intensity by assessing the extent of overlap among areas in which tracked birds spent time at sea and pelagic longline fishing effort derived from AIS, over two distinct spatio-temporal scales. First, we addressed interaction risk over the study area as a binary outcome over seasonal timescales, using seasonal climatologies of ocean data to explore the relative risk of interaction as a function of physical variability (i.e., where and under what conditions birds and fishing overlapped in the average summer over the tracking period). Second, we removed areas in which interaction risk was constantly zero (i.e., no overlap among birds and fisheries) and then modelled the intensity of interaction over monthly timescales using time-matched dynamic ocean data. To compare the usefulness of different metrics of mesoscale turbulence in predicting interaction risk and intensity, we built three separate models for each temporal scale using 1) thermal front frequency (Miller, 2009), 2) FSLE and 3) EKE, and compared model performance.

2.3.1. Residence time of antipodean albatross

We used Residence Time (RT) to estimate the time individuals spent in different locations at sea using the combination of a series of forward and backward first-passage time methods — the time required by an individual to traverse a circle before re-entering it within a given period (Barraquand and Benhamou, 2008). The RT of each individual within each virtual circle with a constant radius was calculated using the function *residenceTime* in the R package *adehabitatLT* (Calenge, 2006). The distance and maximum time between two successive relocations were set to 100 km and 12 h, respectively, matching the resolution of our spatial analysis. The virtual circles with fewer than three relocations were removed, as it was below the minimum number of relocations for calculation. We used RT instead of a predicted probability of occurrence, as generated by other methods (e.g., outputs of a species distribution model or utilisation distributions) to avoid extrapolation of interaction risk (see Section 2.3.4).

2.3.1.1. Daily and monthly occurrence metrics. To derive metrics at daily intervals for individual birds, we rasterised the RT of each individual bird on each day to a 1 × 1° resolution grid using the R package *terra* (Hijmans, 2022). As the calculation of RT for a given diameter considered the whole period of residence (i.e., potentially longer than a day), we divided the RT value (i.e., the number of hours) of each daily rasterised cell by 24 h (Fig. S1). The quotient (i.e., RTP) represented the proportion of a day (spanning 0–1) the individual spent in the grid cell. Values exceeding 1 were corrected to 1. We then estimated daily population RT (*pRT*) by summing the RTP, grouped by age, sex classes and breeding status (i.e., breeder or non-breeder, female adults, male adults or juveniles). Then we summed daily *pRT* of by month for each class of the population to obtain monthly *pRT* (proportion of a day).

2.3.1.2. Weighted average residence time. We assumed that months with more unique tracking days and high *pRT* represent a higher interaction risk for each individual. This would avoid the bias of uneven sample size on different days and from different age classes (i.e., a large sample size on a single day would inflate the total monthly *pRT* if it was directly summed), while avoiding smoothing out potential hotspots by using the median of the *pRT*. Therefore, we calculated the Weighted average Residence Time (WaRT) (days individual^{-1}) in each grid cell by dividing the monthly pRT_{dij} by the monthly total number of individuals, $N_{ind,\ jmd}$, and multiplying it by the number of unique tracking days, U_{jm}:

$$WaRT_{jm} = \frac{U_{jm}}{\sum_{d=1}^{y_m} N_{ind,jmd}} \times \sum_{d=1}^{y_m} \sum_{i=1}^{N_{ind,jmd}} pRT_{dij}$$

where *pRT* is the daily sum RTP of the population *i* in grid cell *j* on a given day *d;* N_{ind} is the daily total number of individuals in population *i* in grid cell *j* on a given day *d* in month *m*; y_m is the number of days in month *m*; U_{jm} is the number of unique tracking days in a given month *m*.

Finally, we normalised the metric of residence time by dividing each WaRT by the number of days in the respective month y_m, to derive the metric for monthly WaRT (mWaRT) in grid cell *j* of a given month *m*:

$$\mathrm{mWaRT}_{jm} = \mathrm{WaRT}_{jm} / y_m$$

This is a continuous value (0–1) that represents the incidence of occurrence in proportion to each month (i.e., fraction of the month per individual). For example, if the mWaRT = 0.8 in grid cell *j* in January (i.e., 31 days) for juveniles, the estimated incidence of occurrence is 24.8 days or 595.2 h per individual. mWaRT was used for estimating interaction risk and statistical modelling at the monthly level in Sections 2.3 and 2.4.

2.3.2. Monthly interaction intensity

We calculated the Interaction Risk (IR) metric as the product of the monthly total fishing hours (hours per 100 km^2 per month) and mWART (fraction of month per individual) for each life-history stage. This yields a spatial exposure index, representing the cumulative fishing effort likely to be encountered per individual per grid cell in each month (hours per individual).

2.3.3. Seasonal interaction risk

For albatross' residence time at seasonal and population levels, we first calculated the WaRT each year by repeating the procedure in *2.3.1.1* and *2.3.1.2*, but substituting the months with seasons (e.g., Austral winter; June–August). Thus, we had the seasonal WaRT (sWaRT) for each year. For fishing effort, we summed the total fishing hours of the three months of the respective seasons in each year. Finally, for seasonal interaction risk (sIR), we first calculated the IR of each season as the product of sWaRT and seasonal total fishing hours. Then we converted the metrics into binary (0 or 1), in which sIR = 1 referred to the presence of co-occurrence, while sIR = 0 referred to the absence of either birds, fishing effort, or both. Albatrosses were grouped by their breeding status (i.e., juvenile, breeder and non-breeder) in the calculation of seasonal occurrence due to computational limits (explained further in Section 2.4).

2.3.4. Dynamic time-matched predictors

The monthly and seasonal averages of dynamic variables and mesoscale turbulence and other static environmental variables (e.g., seafloor depth (Depth; m), bird characteristics) were then spatially matched with the interaction risk of each grid. The monthly medians and static variables were then time-matched with the monthly IR metrics of each grid cell, while the seasonal medians were time-matched with the seasonal IR metrics of each grid cell. MLD and Chl-a were log-transformed before running the spatial models.

2.4. Modelling

2.4.1. Seasonal interaction risk

To assess the influence of physical variability on seasonal interaction risk, we ran binomial GAMs with a logistic link function using the R package mgcv, with seasonal climatological ocean data as predictor variables (Wood, 2006, 2017). Each predictor variable was smoothed by season, and knots were restricted to 5 to avoid overfitting (Wood et al., 2016). We resampled the data for 100 iterations by randomly selecting locations of presence (i.e., grids with positive IR values) and absence (i.e., grids with no IR) in the ratio of 1:2 to identify the underlying biophysical structure of the locations with interaction risk from the background (i.e., areas without interaction risk). Of the biological variables, only breeding status was included in the model as a factor variable due to computational limits. In each iteration, we split our data into a training set for modelling (80 % of the data), with the remaining 20 % used as a test set. To compare these different sets of candidate models, we used Aikaike's Information Criterion (AIC) (Akaike, 1974; Burnham and Anderson, 2002). Underestimation error in spatial prediction, overestimated model performance and overestimated predictive power are common to conventional random selection of non-spatially independent training and testing folds (Roberts et al., 2017; Hao et al., 2019; Valavi et al., 2019) To further evaluate the performance of our seasonal predictive models, we also used the Area Under the Receiver Operating Characteristic Curve (AUC_{ROC}) to measure the discriminatory ability of our predictive binary models of the presence of interaction among seasons (Hanley and McNeil, 1982). The AUC ranges from 0 to 1, where random classification is indicated by 0.5 and perfect classification is indicated by 1 (Hanley and McNeil, 1982). The higher the AUC score, the better the ability of the model.

2.4.2. Monthly interaction intensity

To assess the influence of dynamic ocean conditions on the intensity of interaction risk, we first ran a conditional inference tree (CIT) using interaction risk as the response variable and ocean variables as predictors to look for strong signals of zero interaction risk over large areas. Zero risk results from either (or both) an absence of fishing effort (i.e., cells in which fishing was never recorded) or an absence of Antipodean albatross tracks (i.e., cells in which albatrosses were never recorded). We removed regions of constant zero risk from the dataset according to the CIT result. By CIT, we were able to retain 0 s that are ecologically and statistically informative/ meaningful and alleviate zero-inflation. The remaining 0 s were pseudo-absence locations that occurred within environmental ranges that were also associated with non-zero IR, which were the absences under similar environmental conditions where albatross-fishing interactions were observed elsewhere. This helped restrict the study area to study the intensity of co-occurrence in our models and help differentiate conditions with and without interaction.

For each monthly model of a unique mesoscale turbulence as predictor variables (i.e., either front frequency, FSLE or EKE), we also included all other environmental predictors and used age, sex and breeding status as categorical factors (Table 2). We used generalised additive models (GAMs) with a Tweedie family. The Tweedie

distribution is useful for analysing non-normally distributed data containing large proportions of zeros (Tweedie, 1984; Wood et al., 2016). By the nature of spatial overlapping, the finer the scale of assessment, the smaller the indices of overlap become (Croxall et al., 2013). Thus, our continuous IR metric was positive-valued and continuous but skewed toward zero because of the fine temporal scale. The distribution parameter in the Tweedie family was set to 1.9 (i.e., close to the Gamma distribution) after trials. We used thin-plate regression spline smoothers, which allow a strong enough penalisation to shrink the coefficient of the smoother to zero, where warranted by the data (Marra and Wood, 2011). We compared the models based on Aikaike's Information Criterion (AIC) and the percentage of deviance explained to select the best explanatory models (Akaike, 1974; Burnham and Anderson, 2002).

3. Results

3.1. Seasonal space use

The occurrence at sea for the albatrosses varied seasonally and between sex and age classes (Fig. 2a). For juveniles, the highest occurrence (31–75 days per individual) was observed around the eastern New Zealand EEZ border in austral autumn (i.e., March, April and May) and winter (i.e., June, July and August) between 35°S to 45°S. Otherise, their occurrence was mainly found in the Tasman Sea between 30°S to 40°S, with 16–30 days in austral spring (i.e., September, October and November) and winter, and along the east coast of New Zealand (37.5°S to 47.5° S), with 16–30 days from austral summer (i.e., December, January and February) to winter (Fig. 2a). Seasonal variation in WaRT was more obvious for both females and males, where the highest occurrence was found in winter for both sex groups. Commonly for both groups, the highest occurrence was found along the east coast of New Zealand close to the EEZ border (40°S to 47.5°S), with 6–15 days for females and 16–30 days for males in winter. High occurrence was found near the breeding colony for breeders (Fig. S2) and along the Chilean coast for non-breeders (Fig. S2). In contrast, females had a high occurrence in the Tasman Sea during winter and spring, but males did not. Males occurred further southward compared to the other two groups.

3.2. Fisheries interaction risk

3.2.1. Pelagic longline fishing effort

Pelagic longline fishing effort in our study area (22.5°S – 44.5°S) peaked from autumn to spring (Fig. 2b). Apart from the Australian east coast and the east coast of North Island of New Zealand, four regions of high fishing effort were identified in the high seas (Fig. 2b): the Tasman Sea (150° to 170°), between Norfolk Island and New Zealand (170° to 180°), the south Pacific adjacent to the east of New Zealand EEZ (175° to 147°), and the southwestern-central Pacific (230° to 270°). The highest fishing effort was found near 30°S. However, fishing effort shifted further south in autumn and winter.

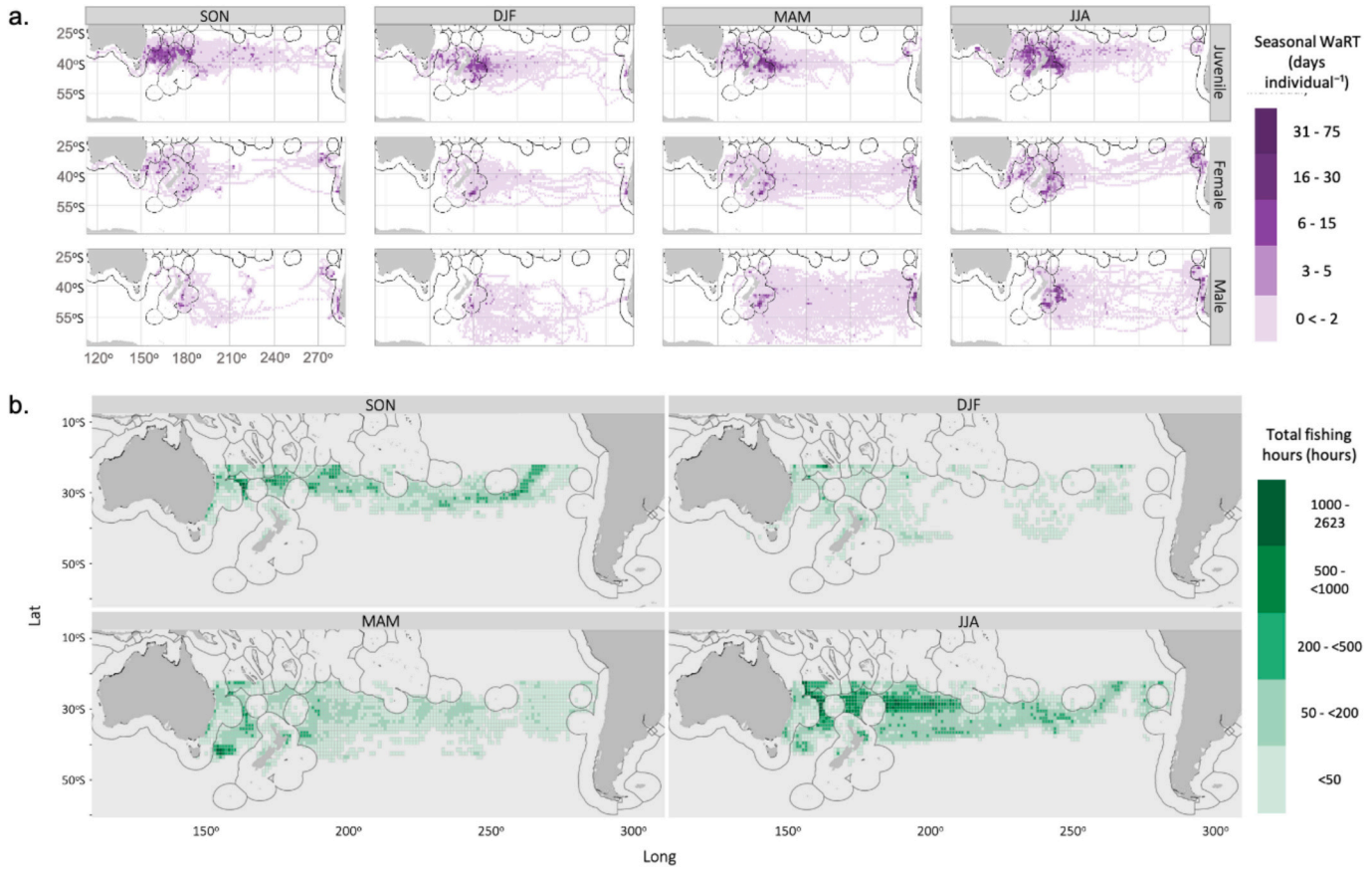

Fig. 2. (a) Seasonal Weighted average Residence Time (WaRT) of Antipodean Albatross across seasons, grouped by sex and age (i.e., juvenile, female and male adult). (b) Average total pelagic longline fishing hours per 100 km^2 from Global Fishing Watch within the study area (i.e., flight range of tracked Antipodean albatross). Each 1° x 1° cell, grouped by austral season (i.e., spring - SON; summer - DJF; autumn - MAM; winter - JJA), represents the average residence time (i.e., day per individual) by the purple gradient (i.e., dark purple indicate higher WaRT) in proportion to the respective quarter of the year or, the median of the 3-month total fishing hours (i.e., hours) by green gradient (i.e., dark green indicates higher total fishing hours) each year across the study period (2019–2022). Thin grey lines represent the exclusive economic zones (EEZs). (For interpretation of the references to color in this figure legend, the reader is referred to the web version of this article.)

3.2.2. Hotspots of albatross–fisheries interaction risk

Overall, hotspots of interaction risk for females, males and juveniles were identified in four regions (Fig. 3, Fig. S3). They were (i) the Tasman Sea (150°–170°E), (ii) the east coast of North Island of New Zealand EEZ, (iii) the South Pacific High Seas adjacent to the east of New Zealand EEZ (185°–213°) and, (iv) the southwestern-central Pacific High Seas (230°–270°) in the mid-latitudes (Fig. 3).

Seasonal variation in interaction risk was observed among all life-history stages in the Antipodean albatross. The average interaction risk was the highest in the autumn and winter (Fig. 3). Our analysis revealed multiple variations in interaction-risk hotspots among the age classes, seasonally and geographically. Seasonally, juveniles had relatively higher interaction risk than adults throughout the year, whereas among adults, the interaction risk was lower in spring and summer (Fig. 3), when fishing effort reduced south of 30°S (Fig. 2b). Geographically, a few interaction hotspots were distinctive to juveniles (e.g., the High Seas of southeast Pacific in the mid-latitudes (25°S–30°S) in winter, and southwest central Pacific in spring and winter (230°–270°)) (Fig. 3). For different life-history stages, hotspots of interaction risk for breeders were found in autumn and winter, and sporadically in the Tasman Sea for females (Fig. S3). As for non-breeders, hotspots of interaction risk were concentrated in the Tasman Sea and along the east coast of North Island, New Zealand for females and spread in the southern and southwestern-central Pacific High Seas. The intensity of interaction risk varied between sexes, where the interaction risk for female non-breeders was higher than for male non-breeders.

3.3. Influence of Mesoscale Ocean dynamics

3.3.1. Seasonal interaction risk

The strongest predictor of the likelihood of the presence of interaction risk of all breeding classes in the best explanatory model was thermal-front frequency, based on its lowest average AIC score (6614.96, 95 % CI [6598.48, 6631.45], ΔAIC = −15.5 to −18.1) and the percentage of deviance explained (37.83 %, 95 % CI [37.72 %, 37.95 %]) (Table S1). It was the most informative mesoscale metric in explaining where interactions are most likely to occur across climatological seasons. The AUC was consistent among the models (0.87), showing the model's ability to correctly classify the response (Table S1). The likelihood of interaction was positively associated with front frequency, with a steady increase from 40 % (Fig. 4a). The likelihood followed the same pattern across different breeding classes. Interactions were most likely to occur at 60–70 % in autumn and 65–75 % in winter. Interaction risk was associated with SST but with seasonal variation (Fig. 4a). A higher chance of interaction risk was expected when SST was relatively warm (i.e., at 18–22.5 °C in autumn, and 15–17 °C in winter). Chlorophyll-*a* and seafloor depth were also associated with interaction risk, with complementary effects (Fig. S4). Chlorophyll-*a* was positively associated with IR in Spring and Autumn. A bimodal pattern was shown from seafloor depth, highlighting two regions where IR was elevated (i.e., from −1000 to −2000 m and −4500 to 5500 m).

3.3.2. Interaction intensity

FSLE was the strongest predictor of monthly intensity of interaction risk in the best explanatory model, having the lowest AIC score and the highest deviance explained (23.5 %) among the three mesoscale monthly Tweedie GAMs (Table 3). The intensity of interaction risk was associated with aggregative LCS, indicated by negative FSLE (Fig. 4b). The intensity of interaction risk was positively associated with all other dynamic oceanographic variables. We found that the intensity of interaction risk was higher during May–August and for SSTs of 14–22 °C, Chl-*a* of 0.1–0.2 mg/m^3 and MLD deeper than 40 m (Fig. 4b). Front frequency and EKE were less informative for the intensity of interaction risk on a finer scale; the latter's contribution to the explanation of deviance was shrunk close to zero in the model by the default selection function.

4. Discussion

Our findings reveal that mesoscale ocean dynamics structure the predictability of fisheries interactions for an endangered seabird. Over seasonal scales, thermal front frequency is a useful predictor of overlap with pelagic longline fishing effort, particularly in the austral autumn and winter. Over finer, monthly scales, aggregative Lagrangian coherent structures elevated the intensity of interaction, with a greater interaction risk associated with more strongly aggregative surface features, from May to August. Juvenile Antipodean albatross had the highest interaction risk of all life-history stages throughout the annual cycle in our study. These findings provide new insight into the influence of dynamic seascapes on the likelihood of interactions between seabirds and pelagic longline fisheries, providing opportunities for managers to better

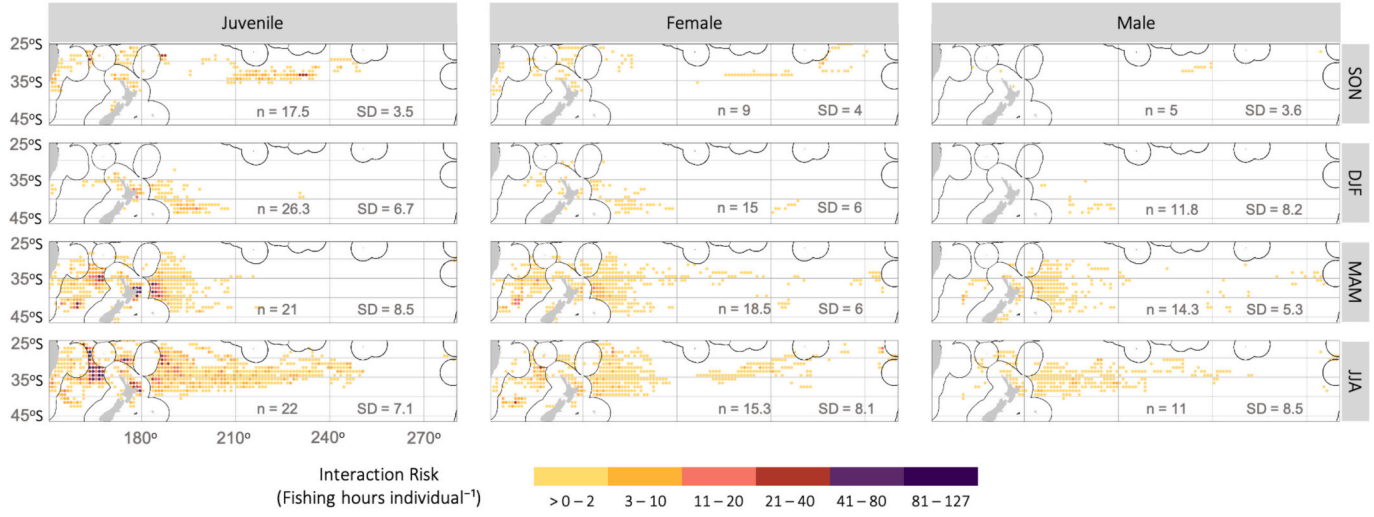

Fig. 3. Seasonal average interaction risk (IR), mean number of individuals (n) and standard deviation (SD) of Antipodean Albatross, grouped by sex and age (i.e., juvenile, female and male adult). Each 1° x 1° cell represents the mean of seasonal interaction risk (i.e., fishing hours individual^{-1}) by the color gradient from yellow to dark purple (i.e., the dark shade indicates the higher IR) across the study period (2019–2022) within each austral season (i.e., spring – SON; summer – DJF; autumn – MAM; winter – JJA). (For interpretation of the references to color in this figure legend, the reader is referred to the web version of this article.)

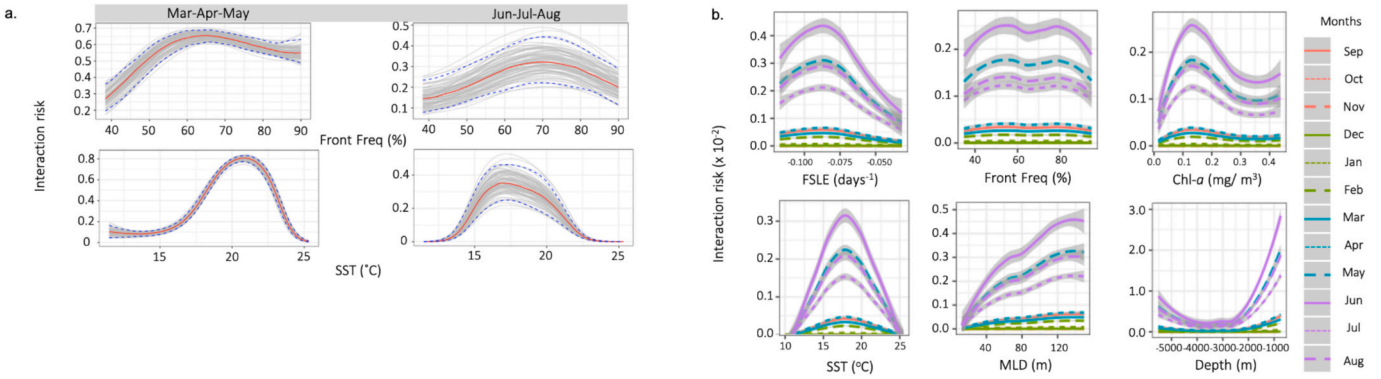

Fig. 4. Response curves of predictor variables in the best Generalised Additive Models of juvenile Antipodean albatross: (a) seasonal likelihood of interaction risk in austral autumn (March to May) and winter (June to August); (b) monthly intensity of interaction risk where colors indicate season and linetypes represent the month in the respective season. Variables include thermal front frequency (Front Freq), Finite-sized Lyapunov Exponent (FSLE), sea surface temperature (SST), chlorophyll-*a* (Chl-*a*), water depth, and mixed layer depth (MLD).

Table 3
Best explanatory monthly Tweedie Generalised Additive Models (GAM) to study the predictors of the monthly intensity of interaction risk.

Mesoscale signal	Parametric coefficients	Estimate	Std. error	t value	Pr(>|t|)	Deviance explained	AIC (ΔAIC)
FSLE	(Intercept)	−11.21	0.44	−25.72	< 2e-16		
	Approximate significance of smooth terms	edf	Ref.df	F	*p*-value		
	FSLE	4.569	9	1.295	0.0023		
	SST	8.648	9	32.03	< 2e-16	23.5 %	23,138
	log10(MLD)	8.450	9	14.98	< 2e-16		(± 0)
	log10(Chl-*a*)	7.039	9	5.918	< 2e-16		
	Bathymetry	8.038	9	8.306	< 2e-16		
	month	8.649	9	88.005	< 2e-16		
	Year	2.890	3	11.895	< 2e-16		
Front Freq	(Intercept)	−11.19	0.43	−26.13	< 2e-16	23.5 %	23,218
	Approximate significance of smooth terms	edf	Ref.df	F	p-value		(+ 80)
	Front Freq	5.452	9	1.742	0.002		
	SST	8.678	9	27.558	< 2e-16		
	log10(MLD)	8.488	9	12.261	< 2e-16		
	log10(Chl-*a*)	6.230	9	4.445	< 2e-16		
	Bathymetry	8.327	9	9.016	< 2e-16		
	month	8.620	9	86.892	< 2e-16		
	Year	2.885	3	10.152	< 2e-16		
EKE	(Intercept)	−11.14	0.44	−25.07	< 2e-16		
	Approximate significance of smooth terms	edf	Ref.df	F	p-value		
	log10(EKE)	0.66	9	0.082	0.291		
	SST	8.635	9	28.227	< 2e-16	23.1 %	23,271
	log10(MLD)	8.544	9	21.101	< 2e-16		(+ 133)
	log10(Chl-*a*)	6.750	9	8.497	< 2e-16		
	Bathymetry	8.006	9	7.923	< 2e-16		
	month	8.621	9	91.782	< 2e-16		
	Year	2.891	3	12.716	< 2e-16		

anticipate dynamic risk zones.

4.1. Age-sex variation of interaction risk hotspots

Hotspots of interaction risk for juveniles were more widespread than for adults, throughout the annual cycle. In other systems, it has been hypothesised that juveniles have a greater bycatch risk due to dispersing more widely than migrating adults (Weimerskirch et al., 2006; Trebilco et al., 2008; Frankish et al., 2020). Our results align with this hypothesis, and with previous work that showed increased exposure to fishing activity for juvenile grey-headed albatross (Frankish et al., 2021). Juveniles spent more time at lower latitudes (25°S–40°S) than adults in the High Seas and Tasman Seas, where fishing effort was higher. The same pattern has been shown by a point-based overlap study evaluating spatiotemporal overlap for both Gibson's and Antipodean Albatross (Rowley et al., 2024).

In our study, the Tasman Sea is the region with the highest interaction risk. While the hotspots of interaction risk in the Tasman Sea were common for juveniles and female non-breeders, they differed in intensity and latitude (i.e., juveniles had higher interaction risk, especially at lower latitudes). Juvenile albatross and petrel species often forage in areas distant from adults (Gutowsky et al., 2014; Pettex et al., 2019; Frankish et al., 2020). This may be a strategy to avoid competition for resources, but the hypothesis has rarely been tested. Nevertheless, the Tasman Sea supports higher primary productivity than the nearby regions in the South Pacific Ocean, with the largest non-coastal chlorophyll-*a* concentration, driven by the convergence of the East Australian Current and the Tasman Front (Tilburg et al., 2002), which may explain the aggregation of both pelagic predators and fishing effort.

Our results also confirm sex-specific variation of hotspots of interaction risk, particularly, the higher interaction risk for females on the east coast of the North Island in the New Zealand EEZ, which aligns with bycatch reports from the New Zealand government (Fisheries New Zealand, 2024). Higher mortality of female adults has been identified by the population model as the major cause of the decline of the Antipodean albatross population (Richard, 2021; Richard et al., 2024). Indeed,

variation in sex or age bycatch ratios has been shown globally (Gianuca et al., 2017). Considering the difference in interaction risk, the impact of bycatch poses threats to the population and life-history stages to different extents. While our results indicate that juveniles had the highest interaction risk at the same hotspots, fewer instances of bycatch of juveniles have been historically reported. This pattern might be because juvenile bycatch may occur mostly beyond the New Zealand EEZ, where monitoring was less comprehensive. Bycatch rates (as opposed to the interaction risk) may simply differ between age classes despite the spatial overlap. Bycatch rates, as a consequence of spatio-temporal overlap with fishing effort, by age–sex class, warrant further study.

It is important to note that spatial overlap does not equate to an encounter or an actual bycatch events. Iteraction risk (i.e., model-derived likelihood of interaction based on the drivers of spatial overlap) — can only be used as a proxy or indicator for bycatch risk or an actual bycatch event. Several factors affect the actual risk of bycatch events occurring, despite the high interaction risk estimated using spatial overlap. First, the timing of the setting of longline hooks is a crucial factor. Albatrosses do not tend to forage after dark, although some are known to "sit-and-wait" forage on the ocean surface (Phalan et al., 2007; Bentley et al., 2021). The temporal scale of our metrics could not capture the difference in interaction risk between day and night. An analysis at a much finer temporal scale, which accounts for day–night differences, would complement our results and provide insights relevant to measures such as night-setting as an effective bycatch mitigation method (Kroodsma et al., 2023). Second, behavioural factors also influence the risk. Aalbatrosses of different age classes vary in their foraging skills and experience (Phillips et al., 2017). Young pelagic seabirds are less experienced and less skilful foragers (Harris et al., 2014; Phillips et al., 2017), which may further increase their risk of becoming entangled or hooked by fishing gear where interaction risk is high. On the other hand, adults are more frequently attracted to fishing boats (Gianuca et al., 2017), at distances of up to 30 km (Collet et al., 2015). Attraction rates rise through immaturity to adulthood in albatrosses (Weimerskirch et al., 2023). Few fine-scale studies have investigated changes in the foraging behaviour of albatrosses in proximity to fishing vessels (Torres et al., 2011; Collet and Weimerskirch, 2020; Corbeau et al., 2021) . However, foraging behaviour has been shown to increase when albatrosses are within 3 km of vessels (Collet et al., 2015). We suggest comparing the response of albatross of different age–sex classes to fishing vessels so that the differences in bycatch risk can be accounted for when estimating interaction risk. Indeed, it is hard to incorporate fine-scale factors such as behaviours or encounters in the interaction risk estimation using broad-scale spatial overlap. Future studies should consider the complexity of the finer-scale drivers of interaction risk, including behaviour and cognition. However, broad-scale interaction risk metrics developed here may be useful for management and spatial prioritisation, particularly as they allow intra-specific or inter-specific comparison.

4.2. Seasonal variation in interaction risk

Seasonal variation in interaction risk can likely be attributed to the southward shift of fishing effort during autumn and winter (Fig. 2b). Risk of interactions between fisheries and albatrosses occurred predominantly at SSTs of 18–22.5 °C in autumn and 15–17 °C in winter. The latitude of the distribution of albatross was consistent throughout the annual cycle (Fig. 2a). As SST was associated with latitude, hotspots of interaction risk were constrained to between 25°S and 40°S. The SST range of albatross–fisheries overlap hotspots in autumn coincided with the SST range preferred by yellowfin tuna (*Thunnus albacares,* 18–31 °C) (Pecoraro et al., 2017). Yellowfin tuna, bigeye tuna (*Thunnus obesus*) and albacore tuna (*Thunnus alalunga*) — the three most popular species for commercial longline fisheries — have broad seasonal distributions extending from 30 to 40°S, with varying degrees of latitudinal and longitudinal dispersion (Williams et al., 2012; Nikolic et al., 2017; SPC-OFP, 2017, 2018; Moore et al., 2020). However, in winter, the SST range of overlapping hotspots was cooler than the thermal threshold of endothermic tuna (Moore et al., 2020). The southward shift of fishing effort in that period could be explained by another popular target of longline fisheries in the South Pacific, the broadbill swordfish (*Xiphias gladius*), as it was found to the south (30–40°S) from April to September (Evans et al., 2014).

4.3. Mesoscale drivers of interaction risk

Metrics of mesoscale surface ocean dynamics have been used to identify drivers of habitat selection by marine predators (Scales et al., 2015; Roberts et al., 2016; Cruz et al., 2021) and drivers of fishing activity (Soykan et al., 2014; Crespo et al., 2018) separately, but rarely have these aspects been considered together. Our results show not only increased time spent by albatross in association with thermal frontal zones but also a concurrent intensification of fishing effort. We reveal that over broad scales, regions with a front frequency of 60–70 % in autumn and 65–75 % in winter had the highest likelihood of interaction. Over finer scales, our results align with previous studies, highlighting the importance of aggregative Lagrangian coherent structures in structuring habitat preferences of marine predators (Kai et al., 2009; d'Ovidio et al., 2013; Cotté et al., 2015; Prants, 2022), fisheries catch locations (Prants et al., 2021; Prants, 2022), and fisheries bycatch risk (Scales et al., 2018).

There are a few advantages of our empirical approach for identifying albatross—fisheries interaction hotspots, while we acknowledged the strength of species distribution models (SDMs) (e.g., Breen et al., 2017). SDMs and habitat suitability models could identify the likely presence of untracked individuals and predict potential habitat use beyond known locations revealed by tracking data (Briscoe et al., 2014). However, our framework avoids extrapolation by relying solely on verified presences. We ensure that inferences about co-occurrence are drawn from observed data. This makes our metrics particularly robust for identifying areas of true interaction risk. This links to the second advantage. Our method allows direct interrogation of the oceanographic conditions where co-occurrence is observed instead of predicted. By linking interaction-risk metrics to dynamic environmental features (e.g., mesoscale fronts), we can identify the mechanisms shaping overlap and differentiate patterns across life-history stages or seasonal periods. Finally, seabirds face trade-offs among flight costs, availability and quality of resources (Weimerskirch et al., 1997). Therefore, their preferences in foraging habitats vary among life-history stages and populations (Phillips et al., 2017). They do not necessarily always target areas of the highest long-term frontal frequency. Fisheries also face similar challenges at sea (i.e., effort, catch efficiency and quality). Our approach reveals concurrent aggregation of animals and fishing effort at transient features, which are insights that would be difficult to obtain from models optimised for longer-term suitability rather than fine-scale overlap.

4.4. Implications for conservation and management

We show that the majority of fisheries—interaction hotspots for Antipodean albatross are located in the high seas. The limitations of regulatory mechanisms in the Areas Beyond National Jurisdictions (ABNJ) remain a substantial barrier to tackling fisheries bycatch at the high seas (Dunn et al., 2019). Our results provide important information for bycatch mitigation management by highlighting specific regions and seasons where dynamic ocean processes elevate the likelihood of overlap between Antipodean albatrosses and pelagic longline fisheries. These insights can guide targeted improvements in bycatch mitigation requirements and monitoring coverage across relevant Regional Fisheries Management Organisations (RFMOs).

Hotspots of interaction risk occurred primarily within Western and Central Pacific Fisheries Commission (WCPFC) waters, including the

Tasman Sea (150–170°), the Norfolk Ridge, and the high seas east of the New Zealand EEZ (170–213°). The WCPFC currently mandates only one of three seabird-mitigation options north of 30° S (WCPFC, 2018). Given our finding that juveniles and females experienced the highest interaction risk between 25 and 30° S, a recommendation following from this work would be for the WCPFC to extend the requirement for comprehensive mitigation measures (bird-scaring lines, branch-line weighting, and night-setting) northward to 25° S within the western and central Pacific. Increasing observer or electronic-monitoring coverage in these high-risk zones could also improve compliance assessment and refine risk estimation.

Interaction-risk hotspots also overlapped with the southern band of longline effort (30–40° S), within the Commission for the Conservation of Southern Bluefin Tuna's (CCSBT) range. Because CCSBT vessels often operate under multiple RFMO authorisations, harmonising mitigation standards with strengthened WCPFC measures would ensure consistent protection across jurisdictions. CCSBT could further promote joint observer-data sharing with WCPFC and ACAP (ACAP, 2023), enabling integrated evaluation of bycatch patterns across fleets targeting tuna and swordfish in overlapping zones.

Our analysis identified juvenile-dominant interaction hotspots extending eastward beyond 213° to 270°, into the southeastern Pacific high seas within Inter-American Tropical Tuna Commission (IATTC) waters. Currently, IATTC requires only one mitigation measure in these areas (IATTC, 2011). To reduce exposure of dispersing juveniles, IATTC could adopt best-practice combinations of measures recommended by ACAP and expand observer and electronic-monitoring coverage in the mid-latitude sector between 25 and 35° S. Only 50–75 % of active vessels that were fitted with AIS transceivers and were >24 m in length were represented by GFW data (Kroodsma et al., 2018). An estimate of 24 % of total fisheries-predator overlap was underreported due to AIS gaps (i.e., technical issues and intentional disabling) in the northeast Pacific (Welch et al., 2024). Due to this uncertainty, our estimate of the total number of fishing hours should be considered the minimum fishing effort.

Across RFMOs, incorporating indicators of mesoscale ocean dynamics—such as thermal-front frequency and Lagrangian-coherent-structure indices—into monitoring frameworks could improve the anticipation of bycatch-risk zones. This could support the development of decision-support tools for dynamic mangement (e.g., near-real-time "nowcast" maps) that allow fleets and managers to adjust operations in response to shifting environmental risk (e.g., Hazen et al., 2018).

Fisheries bycatch remains the foremost threat to the Antipodean albatross and many other seabird species into the future. Consequently, the work we present contains the necessary information to advise management authorities, such as RFMOs, regarding potential adjustments to the current bycatch mitigation requirements and to enable managers to implement targeted measures to slow the population decline of this endangered species. Dynamic ocean management may be a suitable tool to address this challenge in future. Our results reveal that mesoscale ocean dynamics can predict the locations of seabird–fishery overlap hotspots, for different age and sex classes. The approaches we present apply to a wide range of other species and systems and could support the development of more spatiotemporally dynamic management measures, such as near-real-time ("nowcast") decision-support tools (e.g., Hazen et al., 2018; Barlow and Torres, 2021). Crucially, our findings indicate that including measures of mesoscale dynamics when building nowcasting or forecasting systems for fisheries applications could enhance model skill, and therefore the ultimate utility of decision-support tools for industry, managers, communities, and conservation practitioners.

CRediT authorship contribution statement

Ho Fung Wong: Writing – original draft, Methodology, Formal analysis, Conceptualization. **David Schoeman:** Writing – review & editing, Supervision. **Peter I. Miller:** Writing – review & editing, Data curation. **Lily Bentley:** Writing – review & editing, Supervision, Conceptualization. **Luke Halpin:** Writing – review & editing, Supervision, Conceptualization. **Johannes H. Fischer:** Writing – review & editing, Resources, Project administration, Funding acquisition, Data curation. **Igor Debski:** Resources, Data curation. **Samhita Bose:** Resources, Data curation. **Graeme Elliott:** Data curation. **Kath Walker:** Data curation. **Kylie L. Scales:** Writing – review & editing, Supervision, Project administration, Methodology, Funding acquisition, Conceptualization.

Declaration of competing interest

The authors declare the following financial interests/personal relationships which may be considered as potential competing interests: Ho Fung Wong reports financial support was provided by Australian Research Council Discovery Early Career Researcher Award (DECRA), DE210100367. Kylie L. Scales reports financial support was provided by Australian Research Council Discovery Early Career Researcher Award (DECRA), DE210100367. Johannes H. Fischer, Igor Debski, Samhita Bose, Graeme Elliot and Kath Walker report financial support was provided by New Zealand Department of Conservation. Johannes H. Fischer reports financial support was provided by Fisheries New Zealand. Johannes H. Fischer reports financial support was provided by Live Ocean. Johannes H. Fischer, Igor Debski, Samhita Bose, Graeme Elliot and Kath Walker report financial support was provided by British Broadcasting Corp. Johannes H. Fischer, Igor Debski, Samhita Bose, Graeme Elliot and Kath Walker report financial support was provided by Southern Seabirds. If there are other authors, they declare that they have no known competing financial interests or personal relationships that could have appeared to influence the work reported in this paper.

Acknowledgements

We acknowledge funding support from the Australian Research Council (ARC) Discovery Early Career Researcher Award (DECRA) 2021 fellowship held by KLS. PIM acknowledges NERC Earth Observation Data Analysis and Artificial-Intelligence Service (NEODAAS) for use of computing resources. We are grateful to Kaitiaki Rōpū ki Murihiku and Kāi Tahu for allowing us to work on Southern Taonga. Successful visits to Antipodes Island were possible thanks to Steve Kafka and the crew of the *Evohe* and Nathan McCrorie and the crew of *Tranquil Image* enabling safe passage. We also thank the hard work of the Quarantine Store of the Murihiku Office of the Department of Conservation, ensuring the continued pest-free status of this unique island.

Appendix A. Supplementary data

A table of summary of seasonal binomial GAM models result (Table S1), a schematic flow chart of important steps in the calculation of the metric of bird occurrence (Fig. S1), A figure of weighted average residence time Antipodean Albatross across seasons, grouped by life-history stage (Fig. S2), a figure of average interaction risk of Antipodean Albatross, grouped by life-history stage (Fig. S3), and the responsive curves of other predictor variables in the seasonal binomial Generalised Additive Models (Fig. S4). The authors are solely responsible for the content and functionality of these materials. Queries (other than the absence of the material) should be directed to the corresponding author. Supplementary data to this article can be found online at https://doi.org/10.1016/j.biocon.2025.111574.

Data availability

Data will be made available on request.

References

Abraham, E.R., Thompson, F.N., 2015. Captures of Antipodean Albatross in Surface Longline Fisheries, in the New Zealand Exclusive Economic Zone, during the 2015–16 Fishing Year.

Abraham, E.R., Richard, Y., Walker, N., Gibson, W., Daisuke, O., Tsuji, S., 2019. Assessment of the Risk of Surface-longline Fisheries in the Southern Hemisphere to Albatrosses and Petrels, for 2016. CCSBT-ERS/19xx/xx.

ACAP, 2023. Updated ACAP advice on reducing the bycatch of albatrosses and petrels in WCPFC fisheries. Agreement on the conservation of albatrosses and petrels (ACAP). Scientific committee nineteenth regular session. WCPFC-SC19-2023/EB-IP-21. https://meetings.wcpfc.int/node/19486.

Akaike, H., 1974. A new look at the statistical model identification. IEEE Trans Automat Contr 19, 716–723.

Anderson, O., Small, C., Croxall, J., Dunn, E., Sullivan, B., Yates, O., Black, A., 2011. Global seabird bycatch in longline fisheries. Endanger. Species Res. 14, 91–106.

Appen, W.J. von, Institute, A.W., Baumann, T., Janout, M., Koldunov, N., Lenn, Y.D., Pickart, R., Scott, R., Wang, Q., 2022. Eddies and the distribution of eddy kinetic energy in the Arctic Ocean. Oceanography. https://doi.org/10.5670/oceanog.2022.122.

Arnold, J.M., Brault, S., Croxall, J.P., 2006. Albatross populations in peril: a population trajectory for Black-browed albatrosses at South Georgia. Ecol. Appl. 16, 419–432.

Avila, I.C., Kaschner, K., Dormann, C.F., 2018. Current global risks to marine mammals: taking stock of the threats. Biol. Conserv. 221, 44–58.

Barlow, D.R., Torres, L.G., 2021. Planning ahead: dynamic models forecast blue whale distribution with applications for spatial management. J. Appl. Ecol. 58, 2493–2504.

Barraquand, F., Benhamou, S., 2008. Animal movements in heterogeneous landscapes: identifying profitable places and homogeneous movement bouts. Ecology 89, 3336–3348.

Bentley, L.K., Kato, A., Ropert-Coudert, Y., Manica, A., Phillips, R.A., 2021. Diving behaviour of albatrosses: implications for foraging ecology and bycatch susceptibility. Mar. Biol. 168, 36.

Boffetta, G., Lacorata, G., Redaelli, G., Vulpiani, A., 2001. Detecting barriers to transport: a review of different techniques. Phys. D Nonlinear Phenom. 159, 58–70.

Breen, P., Brown, S., Reid, D., Rogan, E., 2017. Where is the risk? Integrating a spatial distribution model and a risk assessment to identify areas of cetacean interaction with fisheries in the northeast Atlantic. Ocean Coast. Manag. 136, 148–155.

Briscoe, D., Hiatt, S., Lewison, R., Hines, E., 2014. Modeling habitat and bycatch risk for dugongs in Sabah, Malaysia. Endanger. Species Res. 24, 237–247.

Brough, T., Rayment, W., Slooten, E., Dawson, S., 2019. Fine scale distribution for a population of New Zealand's only endemic dolphin (*Cephalorhynchus hectori*) shows long-term stability of coastal hotspots. Mar. Mamm. Sci. 35, 140–163.

Bugoni, L., McGill, R.A.R., Furness, R.W., 2010. The importance of pelagic longline fishery discards for a seabird community determined through stable isotope analysis. J. Exp. Mar. Biol. Ecol. 391, 190–200.

Burnham, K.P., Anderson, D.R., 2002. Model Selection and Multimodel Inference, A Practical Information-Theoretic Approach, 2004, pp. 267–351.

Calenge, C., 2006. The package "adehabitat" for the R software: a tool for the analysis of space and habitat use by animals. Ecol. Model. 197, 516–519.

Carneiro, A.P.B., et al., 2020. A framework for mapping the distribution of seabirds by integrating tracking, demography and phenology. J. Appl. Ecol. 57, 514–525.

Clay, T.A., Small, C., Tuck, G.N., Pardo, D., Carneiro, A.P.B., Wood, A.G., Croxall, J.P., Crossin, G.T., Phillips, R.A., 2019. A comprehensive large-scale assessment of fisheries bycatch risk to threatened seabird populations. J. Appl. Ecol. 56, 1882–1893.

Collet, J., Weimerskirch, H., 2020. Albatrosses can memorize locations of predictable fishing boats but favour natural foraging. Proc. R. Soc. B Biol. Sci. 287, 20200958.

Collet, J., Patrick, S., Weimerskirch, H., 2015. Albatrosses redirect flight towards vessels at the limit of their visual range. Mar. Ecol. Prog. Ser. 526, 199–205.

Copello, S., Pon, J.P.S., Favero, M., 2014. Spatial overlap of Black-browed albatrosses with longline and trawl fisheries in the Patagonian Shelf during the non-breeding season. J. Sea Res. 89, 44–51.

Corbeau, A., Collet, J., Orgeret, F., Pistorius, P., Weimerskirch, H., 2021. Fine-scale interactions between boats and large albatrosses indicate variable susceptibility to bycatch risk according to species and populations. Anim. Conserv. 24, 689–699. https://doi.org/10.1111/acv.12676.

Cotté, C., d'Ovidio, F., Dragon, A.C., Guinet, C., Lévy, M., 2015. Flexible preference of southern elephant seals for distinct mesoscale features within the Antarctic circumpolar current. Prog. Oceanogr. 131, 46–58.

Crespo, G.O., Dunn, D.C., Reygondeau, G., Boerder, K., Worm, B., Cheung, W., Tittensor, D.P., Halpin, P.N., 2018. The environmental niche of the global high seas pelagic longline fleet. Sci. Adv. 4, eaat3681.

Croxall, J., Small, C., Sullivan, B., Wanless, R., Frere, E., Lascelles, B., Ramirez, I., Sato, M., Yates, O., 2013. Appropriate scales and data to manage seabird-fishery interactions: comment on Torres et al. (2013). Mar. Ecol. Prog. Ser. 493, 297–300.

Cruz, A., Ramos, F., Navarro, G., Cózar, A., Bécares, J., Arroyo, G.M., 2021. Drivers for spatial modelling of a critically endangered seabird on a dynamic ocean area: Balearic shearwaters are non-vegetarian. Aquat. Conserv. Mar. Freshwat. Ecosyst. 31, 1700–1714.

Cruz, A., Rodríguez-García, C., Cabrera-Castro, R., Arroyo, G.M., 2022. Correlation between seabirds and fisheries varies by species at fine-scale pattern. ICES J. Mar. Sci. 80, 2427–2440.

Cury, P.M., et al., 2011. Global seabird response to forage fish depletion—one-third for the birds. Science 334, 1703–1706.

Della Penna, A., Koubbi, P., Cotté, C., Bon, C., Bost, C.-A., d'Ovidio, F., 2017. Lagrangian analysis of multi-satellite data in support of open ocean marine protected area design. Deep-Sea Res. II Top. Stud. Oceanogr. 140, 212–221.

Dias, M.P., Martin, R., Pearmain, E.J., Burfield, I.J., Small, C., Phillips, R.A., Yates, O., Lascelles, B., Borboroglu, P.G., Croxall, J.P., 2019. Threats to seabirds: a global assessment. Biol. Conserv. 237, 525–537.

Douglas, D.C., et al., 2012. Moderating Argos location errors in animal tracking data. Methods Ecol. Evol. 3, 999–1007.

d'Ovidio, F., Fernández, V., Hernández-García, E., López, C., 2004. Mixing structures in the Mediterranean Sea from finite-size Lyapunov exponents. Geophys. Res. Lett. 31. https://doi.org/10.1029/2004gl020328.

d'Ovidio, F., Monte, S.D., Penna, A.D., Cotté, C., Guinet, C., 2013. Ecological implications of eddy retention in the open ocean: a Lagrangian approach. J. Phys. A Math. Theor. 46, 254023.

Dunn, D.C., Maxwell, S.M., Boustany, A.M., Halpin, P.N., 2016. Dynamic ocean management increases the efficiency and efficacy of fisheries management. Proc. Natl. Acad. Sci. 113, 668–673.

Dunn, D.C., et al., 2019. The importance of migratory connectivity for global ocean policy. Proc. R. Soc. B 286, 20191472.

Elliott, G., Walker, K., 2019. Antipodean wandering albatross census and population study on Antipodes Island 2019. Unpublished report to the Department of Conservation, Wellington. https://www.doc.govt.nz/our-work/conservation-services-programme/csp-reports/201819/antipodean-albatross-census-and-population-study-2019/.

Elliott, G., Walker, K., 2020. Antipodean wandering albatross: satellite tracking and population study Antipodes Island 2020. Unpublished report to the Department of Conservation, Wellington. https://www.doc.govt.nz/our-work/conservation-services-programme/csp-reports/201920/antipodean-albatross-satellite-tracking-and-population-study-2020/.

Elliott, G., Walker, K., 2022. Antipodean wandering albatross satellite tracking and population study on Antipodes Island in 2021 and 2022. Unpublished report to the Department of Conservation, Wellington. https://www.doc.govt.nz/our-work/conservation-services-programme/csp-reports/202122/antipodean-wandering-albatross-satellite-tracking-and-population-study-2021/.

Evans, K., Abascal, F., Kolody, D., Sippel, T., Holdsworth, J., Maru, P., 2014. The horizontal and vertical dynamics of swordfish in the South Pacific Ocean. J. Exp. Mar. Biol. Ecol. 450, 55–67.

Fisheries New Zealand, 2024. Retrieved from. https://protectedspeciescaptures.nz/PSCv7/released/antipodean-albatross/surface-longline/all-vessels/eez/2002-03-2020-21/1March2024.

Frankish, C.K., Phillips, R.A., Clay, T.A., Somveille, M., Manica, A., 2020. Environmental drivers of movement in a threatened seabird: insights from a mechanistic model and implications for conservation. Divers. Distrib. 26, 1315–1329.

Frankish, C.K., Cunningham, C., Manica, A., Clay, T.A., Prince, S., Phillips, R.A., 2021. Tracking juveniles confirms fisheries-bycatch hotspot for an endangered albatross. Biol. Conserv. 261, 109288.

Gianuca, D., Phillips, R.A., Townley, S., Votier, S.C., 2017. Global patterns of sex- and age-specific variation in seabird bycatch. Biol. Conserv. 205, 60–76.

Gimeno, M., García, J.A., Afán, I., Aymí, R., Montalvo, T., Navarro, J., 2022. Age-related differences in foraging behaviour at sea and interactions with fishing vessels in an opportunistic urban gull. ICES J. Mar. Sci. 80, 2405–2413.

Granadeiro, J.P., Brickle, P., Catry, P., 2014. Do albatrosses specialize in fisheries waste? Anim. Conserv. 17, 19–26.

Grantham, H.S., et al., 2011. Accommodating dynamic oceanographic processes and pelagic biodiversity in marine conservation planning. PloS One 6, e16552.

Grémillet, D., Lewis, S., Drapeau, L., Lingen, C.D.V.D., Huggett, J.A., Coetzee, J.C., Verheye, H.M., Daunt, F., Wanless, S., Ryan, P.G., 2008. Spatial match–mismatch in the Benguela upwelling zone: should we expect chlorophyll and sea-surface temperature to predict marine predator distributions? J. Appl. Ecol. 45, 610–621.

Güçlüsoy, H., 2008. Damage by monk seals to gear of the artisanal fishery in the Foça Monk Seal Pilot Conservation Area, Turkey. Fish. Res. 90, 70–77.

Gutowsky, S.E., Tremblay, Y., Kappes, M.A., Flint, E.N., Klavitter, J., Laniawe, L., Costa, D.P., Naughton, M.B., Romano, M.D., Shaffer, S.A., 2014. Divergent post-breeding distribution and habitat associations of fledgling and adult Black-footed Albatrosses *Phoebastria nigripes* in the North Pacific. Ibis 156, 60–72.

Hanley, J.A., McNeil, B.J., 1982. The meaning and use of the area under a receiver operating characteristic (ROC) curve. Radiology 143, 29–36.

Hao, T., Elith, J., Guillera-Arroita, G., Lahoz-Monfort, J.J., 2019. A review of evidence about use and performance of species distribution modelling ensembles like BIOMOD. Divers. Distrib. 25, 839–852. https://doi.org/10.1111/ddi.12892.

Harris, S., Rey, A.R., Quintana, F., 2014. Breeding experience and foraging behaviour of Imperial Shags (*Leucocarbo atriceps*) in Argentina. Emu 114, 222–228.

Hazen, E.L., Scales, K.L., Maxwell, S.M., Briscoe, D.K., Welch, H., Bograd, S.J., Bailey, H., Benson, S.R., Eguchi, T., Dewar, H., Kohin, S., Costa, D.P., Crowder, L.B., Lewison, R. L., 2018. A dynamic ocean management tool to reduce bycatch and support sustainable fisheries. Sci. Adv. 4, eaar3001. https://doi.org/10.1126/sciadv.aar3001.

Hijmans, R.J., 2022. Terra: spatial data analysis. https://rspatial.org/terra/.

Hobday, A.J., Hartog, J.R., Spillman, C.M., Alves, O., 2011. Seasonal forecasting of tuna habitat for dynamic spatial management. Can. J. Fish. Aquat. Sci. 68, 898–911.

Hobday, A.J., Maxwell, S.M., Forgie, J., McDonald, J., 2013. Dynamic ocean management: integrating scientific and technological capacity with law, policy, and management. Stan. Envtl. LJ 33, 125.

IATTC, 2011. Resolution to mitigate the impact on seabirds of fishing for species covered by the IATTC. Inter-American tropical tuna commission (IATTC). 82nd meeting

resolution C-11-02. https://www.iattc.org/GetAttachment/6117c3fd-ad66-46fe-8005-f6af18f0ee92/C-11-02-Active_Seabirds.pdf.
Jog, K., Sutaria, D., Diedrich, A., Grech, A., Marsh, H., 2022. Marine mammal interactions with fisheries: review of research and management trends across commercial and small-scale fisheries. Front. Mar. Sci. 9, 758013.
Kai, E.T., Rossi, V., Sudre, J., Weimerskirch, H., Lopez, C., Hernandez-Garcia, E., Marsac, F., Garçon, V., 2009. Top marine predators track Lagrangian coherent structures. Proc. Natl. Acad. Sci. 106, 8245–8250.
Kroodsma, D.A., et al., 2018. Tracking the global footprint of fisheries. Science 359, 904–908.
Kroodsma, D., Turner, J., Luck, C., Hochberg, T., Miller, N., Augustyn, P., Prince, S., 2023. Global prevalence of setting longlines at dawn highlights bycatch risk for threatened albatross. Biol. Conserv. 283, 110026. https://doi.org/10.1016/j.biocon.2023.110026.
Lascelles, B.G., et al., 2016. Applying global criteria to tracking data to define important areas for marine conservation. Divers. Distrib. 22, 422–431.
Lewison, R.L., et al., 2014. Global patterns of marine mammal, seabird, and sea turtle bycatch reveal taxa-specific and cumulative megafauna hotspots. Proc. Natl. Acad. Sci. 111, 5271–5276.
Lewison, R., et al., 2015. Dynamic Ocean management: identifying the critical ingredients of dynamic approaches to ocean resource management. BioScience 65, 486–498.
Liu, M., Lin, M., Turvey, S.T., Li, S., 2019. Fishers' experiences and perceptions of marine mammals in the South China Sea: insights for improving community-based conservation. Aquat. Conserv. Mar. Freshwater Ecosyst. 29, 809–819.
Marra, G., Wood, S.N., 2011. Practical variable selection for generalized additive models. Comput. Stat. Data Anal. 55, 2372–2387.
Marsh, H., O'Shea, T., 2011. Ecology and Conservation of the Sirenia. https://doi.org/10.1017/cbo9781139013277.
Maxwell, S.M., Hazen, E.L., Morgan, L.E., Bailey, H., Lewison, R., 2012. Finding balance in fisheries management. Science 336, 413.
Maxwell, S.M., et al., 2015. Dynamic ocean management: defining and conceptualizing real-time management of the ocean. Mar. Policy 58, 42–50.
Miller, P., 2009. Composite front maps for improved visibility of dynamic sea-surface features on cloudy SeaWiFS and AVHRR data. J. Mar. Syst. 78, 327–336.
Moore, B.R., et al., 2020. Defining the stock structures of key commercial tunas in the Pacific Ocean I: current knowledge and main uncertainties. Fish. Res. 230, 105525.
Navarro-Herrero, L., Saldanha, S., Militão, T., Vicente-Sastre, D., March, D., González-Solís, J., 2024. Use of bird-borne radar to examine shearwater interactions with legal and illegal fisheries. Conserv. Biol. https://doi.org/10.1111/cobi.14224.
Nikolic, N., Morandeau, G., Hoarau, L., West, W., Arrizabalaga, H., Hoyle, S., Nicol, S.J., Bourjea, J., Puech, A., Farley, J.H., Williams, A.J., Fonteneau, A., 2017. Review ofalbacore tuna, Thunnus alalunga, biology, fisheries and management. Rev. Fish Biol.Fish. 27, 775–810. https://doi.org/10.1007/s11160-016-9453-y.
Pardo, D., Forcada, J., Wood, A.G., Tuck, G.N., Ireland, L., Pradel, R., Croxall, J.P., Phillips, R.A., 2017. Additive effects of climate and fisheries drive ongoing declines in multiple albatross species. Proc. Natl. Acad. Sci. 114, E10829–E10837.
Pauly, D., Watson, R., Alder, J., 2005. Global trends in world fisheries: impacts on marine ecosystems and food security. Philos. Trans. R. Soc., B 360, 5–12.
Pecoraro, C., Zudaire, I., Bodin, N., Murua, H., Taconet, P., Díaz-Jaimes, P., Cariani, A., Tinti, F., Chassot, E., 2017. Putting all the pieces together: integrating current knowledge of the biology, ecology, fisheries status, stock structure and management of yellowfin tuna (*Thunnus albacares*). Rev. Fish Biol. Fish. 27, 811–841.
Pettex, E., Lambert, C., Fort, J., Dorémus, G., Ridoux, V., 2019. Spatial segregation between immatures and adults in a pelagic seabird suggests age-related competition. J. Avian Biol. 50.
Phalan, B., Phillips, R., Silk, J., Afanasyev, V., Fukuda, A., Fox, J., Catry, P., Higuchi, H., Croxall, J., 2007. Foraging behaviour of four albatross species by night and day. Mar. Ecol. Prog. Ser. 340, 271–286.
Phillips, R.A., Gales, R., Baker, G.B., Double, M.C., Favero, M., Quintana, F., Tasker, M.L., Weimerskirch, H., Uhart, M., Wolfaardt, A., 2016. The conservation status and priorities for albatrosses and large petrels. Biol. Conserv. 201, 169–183.
Phillips, R., Lewis, S., González-Solís, J., Daunt, F., 2017. Causes and consequences of individual variability and specialization in foraging and migration strategies of seabirds. Mar. Ecol. Prog. Ser. 578, 117–150. https://doi.org/10.3354/meps12217.
Prants, S.V., 2022. Marine life at Lagrangian fronts. Prog. Oceanogr. 204, 102790.
Prants, S.V., Budyansky, M.V., Uleysky, Myu, Kulik, V.V., 2021. Lagrangian fronts and saury catch locations in the Northwestern Pacific in 2004–2019. J. Mar. Syst. 222, 103605.
Read, A.J., Drinker, P., Northridge, S., 2006. Bycatch of marine mammals in U.S. and global fisheries. Conserv. Biol. 20, 163–169.
Richard, Y., 2021. Integrated Population Model of Antipodean Albatross for Simulating Management Scenarios, 31 pages. Technical Report Prepared for Department of Conservation – June 2021.
Richard, Y., Abraham, E.R., 2020. Assessment of the risk of commercial fisheries to New Zealand seabirds, 2006–07 to 2016–17. New Zealand Aquatic Environment and Biodiversity Report No. 237, 61 p. Retrieved from. https://mpi.govt.nz/dmsdocument/39407.
Richard, Y., Berkenbusch, K., Crawford, E., Tornquist, M., Walker, K., Elliott, G., Tremblay-Boyer, L., 2024. Antipodean albatross multi-threat risk assessment. N. Z. Aquat. Environ. Biodivers. Rep. No. 332, 62 p.
Rivalan, P., Barbraud, C., Inchausti, P., Weimerskirch, H., 2010. Combined impacts of longline fisheries and climate on the persistence of the Amsterdam Albatross *Diomedia amsterdamensis*. Ibis 152, 6–18.
Roberts, J.J., et al., 2016. Habitat-based cetacean density models for the U.S. Atlantic and Gulf of Mexico. Sci. Rep. 6, 22615.
Roberts, D.R., Bahn, V., Ciuti, S., Boyce, M.S., Elith, J., Guillera-Arroita, G., et al., 2017. Cross-validation strategies for data with temporal, spatial, hierarchical, or phylogenetic structure. Ecography 40, 913–929. https://doi.org/10.1111/ecog.02881.
Robertson, H.A., Bair, K.A., Elliott, G.P., Hitchmough, R.A., McArthur, N.J., Makan, T.D., Miskelly, C.M., O'Donnell, C.F.J., Sagar, P.M., Scofield, R.P., Taylor, G.A., Michel, P., 2021. Conservation status of birds in Aotearoa New Zealand, 2021. In: New Zealand Threat Classification Series 36. Department of Conservation, Wellington, 43 p.
Rowley, O., Waipoua, T.A., Debski, I., Elliot, G., Parker, G., Rexer-Huber, K., Walker, K., Fischer, J., 2024. Fine scale overlap analysis of Antipodean and Gibson's albatross with Pelagic Longline Fishing Effort. Agreement on the Conservation of Albatrosses and Petrels Joint Twelfth Meeting of the Seabird Bycatch Working Group and Eighth Meeting of the Population and Conservation Status Working Group. Joint SBWG12/PaCSWG8 Doc 07 Agenda Item 3.1, 4.1.
Scales, K., Miller, P., Varo-Cruz, N., Hodgson, D., Hawkes, L., Godley, B., 2015. Oceanic loggerhead turtles Caretta caretta associate with thermal fronts: evidence from the Canary Current Large Marine Ecosystem. Mar. Ecol. Prog. Ser. 519, 195–207.
Scales, K.L., Hazen, E.L., Jacox, M.G., Castruccio, F., Maxwell, S.M., Lewison, R.L., Bograd, S.J., 2018. Fisheries bycatch risk to marine megafauna is intensified in Lagrangian coherent structures. Proc. Natl. Acad. Sci. 115, 7362–7367.
Slooten, E., Dawson, S.M., 2010. Assessing the effectiveness of conservation management decisions: likely effects of new protection measures for Hector's dolphin (*Cephalorhynchus hectori*). Aquat. Conserv. Mar. Freshw. Ecosyst. 20, 334–347.
Soykan, C.U., Eguchi, T., Kohin, S., Dewar, H., 2014. Prediction of fishing effort distributions using boosted regression trees. Ecol. Appl. 24, 71–83.
SPC-OFP, 2017. Project 42: Pacific tuna tagging project report and workplan for 2017–2020. In: Research Project Report WCPFC-SC13-2017/RP-PTTP-02 Presented to the Thirteenth Regular Session of the Scientific Committee of the Western and Central Pacific Fisheries Commission. Cook Islands, Rarotonga.
SPC-OFP, 2018. Project 42: Pacific tuna tagging project report and workplan for 2018–2021. In: Research Project Report WCPFC-SC12-2018/RP-PTTP-02 Presented to the Fourteenth Regular Session of the Scientific Committee of the Western and Central Pacific Fisheries Commission. Busan, Republic of Korea.
Tilburg, C.E., Subrahmanyam, B., O'Brien, J.J., 2002. Ocean color variability in the Tasman Sea. Geophys. Res. Lett. 29, 125–1–125–4.
Torres, L., Thompson, D., Bearhop, S., Votier, S., Taylor, G., Sagar, P., Robertson, B., 2011. White-capped albatrosses alter fine-scale foraging behavior patterns when associated with fishing vessels. Mar. Ecol. Prog. Ser. 428, 289–301.
Trebilco, R., Gales, R., Baker, G.B., Terauds, A., Sumner, M.D., 2008. At sea movement of Macquarie Island giant petrels: relationships with marine protected areas and regional fisheries management Organisations. Biol. Conserv. 141, 2942–2958.
Tweedie, M.C.K., Ghosh, J.K., Roy, J., 1984. An index which distinguishes between some important exponential families. Statistics: applications and new directions. In: Proceedings of the Indian Statistical Institute Golden Jubilee International Conference. Indian Statistical Institute, Calcutta, pp. 579–604.
Valavi, R., Elith, J., Lahoz-Monfort, J.J., Guillera-Arroita, G., 2019. blockCV: an R package for generating spatially or environmentally separated folds forK-fold cross-validation of species distribution models. Methods Ecol. Evol. 10, 225–232. https://doi.org/10.1111/2041-210X.13107.
Véran, S., Gimenez, O., Flint, E., Kendall, Wl, Jr, Pfd, Lebreton, J., 2007. Quantifying the impact of longline fisheries on adult survival in the black-footed albatross. J. Appl. Ecol. 44, 942–952.
Votier, S.C., Furness, R.W., Bearhop, S., Crane, J.E., Caldow, R.W., Catry, P., Ensor, K., Hamer, K.C., Hudson, A.V., Kalmbach, E., Klomp, N.I., Pfeiffer, S., Phillips, R.A., Prieto, I., Thompson, D.R., 2004. Changes in fisheries discard rates and seabird communities. Nature 427 (6976), 727–730. https://doi.org/10.1038/nature02315.
Votier, S.C., Sherley, R.B., Scales, K.L., Camphuysen, K., Phillips, R.A., 2023. An overview of the impacts of fishing on seabirds, including identifying future research directions. ICES J. Mar. Sci. 80, 2380–2392.
Wanless, R.M., Ryan, P.G., Altwegg, R., Angel, A., Cooper, J., Cuthbert, R., Hilton, G.M., 2009. From both sides: dire demographic consequences of carnivorous mice and longlining for the critically endangered Tristan albatrosses on Gough Island. Biol. Conserv. 142, 1710–1718.
WCPFC, 2018. Conservation and Management Measure to mitigate the impact of fishing for highly migratory fish stocks on seabirds. Western and Central Pacific Fisheries Commission (WCPFC) Conservation and Management Measure 2018-03. https://cmm.wcpfc.int/measure/cmm-2018-03.
Weimerskirch, H., Cherel, Y., Cuenot-Chaillet, F., Ridoux, V., 1997. Alternative foraging strategies and resource allocation by male and female wandering albatrosses. Ecology 78, 2051.
Weimerskirch, H., Åkesson, S., Pinaud, D., 2006. Postnatal dispersal of wandering albatrosses Diomedea exulans: implications for the conservation of the species. J. Avian Biol. 37, 23–28.
Weimerskirch, H., Filippi, D.P., Collet, J., Waugh, S.M., Patrick, S.C., 2018. Use of radar detectors to track attendance of albatrosses at fishing vessels. Conserv. Biol. 32, 240–245.
Weimerskirch, H., Corbeau, A., Pajot, A., Patrick, S.C., Collet, J., 2023. Albatrosses develop attraction to fishing vessels during immaturity but avoid them at old age. Proc. R. Soc. B 290, 20222252.
Welch, H., Clavelle, T., White, T.D., Cimino, M.A., Kroodsma, D., Hazen, E.L., 2024. Unseen overlap between fishing vessels and top predators in the northeast Pacific. Sci. Adv. 10, eadl5528.
Williams, A.J., Farley, J.H., Hoyle, S.D., Davies, C.R., Nicol, S.J., 2012. Spatial and sex-specific variation in growth of albacore tuna (*Thunnus alalunga*) across the SouthPacific Ocean. PloS One 7, e39318. https://doi.org/10.1371/journal.pone.0039318.

Wood, S.N., 2006. Generalized Additive Models. https://doi.org/10.1201/9781420010404.
Wood, S.N., 2017. Generalized additive models, An Introduction with RDOI. https://doi.org/10.1201/9781315370279.
Wood, S.N., Pya, N., Säfken, B., 2016. Smoothing parameter and model selection for general smooth models. J. Am. Stat. Assoc. 111, 1548–1563.